Journal of Physics: Conference Series **355** (2012) 012027 doi:10.1088/1742-6596/355/1/012027

Influence of the cosmological evolution of the EBL on the limits derived from VHE gamma-ray blazar observations

Manuel Meyer[1], **Martin Raue**[1] **and Daniel Mazin**[2]

[1]Institut für Experimentalphysik, University of Hamburg, Luruper Chaussee 149, 22767 Hamburg, Germany
[2]Institut de Fisica d'Altes Energies (IFAE), Edifici Cn. Universitat Autonoma de Barcelona, 08193 Bellaterra, Spain

E-mail: manuel.meyer@physik.uni-hamburg.de

Abstract. Very high energy (VHE) γ-rays from distant sources such as blazars are attenuated due to the interaction with low energy photons of the extragalactic background light (EBL) in the ultraviolet to infrared wavelength band. Thus, the EBL leaves an imprint on the observed energy spectra of such sources. With assumptions about the source physics it is possible to derive limits on the EBL photon density. However, the EBL evolves with redshift a fact that often been neglected in the deviations of the limits. Here, the influence of evolution is examined by implementing it in a phenomenological way with four VHE spectra and compared to previous results.

1. Introduction

The extragalactic background light (EBL) is the diffuse isotropic background radiation field that ranges from ultraviolet / optical to far infrared wavelengths. The two main contributions to this radiation field are emitted starlight integrated over all epochs and the starlight absorbed and re-emitted by dust in galaxies [1, for a review]. Further possible components that add to the total EBL intensity are active galactic nuclei (AGN) [2], the very first (population III) stars [3] or even exotic candidates such as dark matter powered stars [4]. Knowledge of the spectral energy distribution (SED) of the EBL allows for insight of the cosmic star and galaxy formation rates as well as the amount of dust contained in galaxies. The EBL is however difficult to measure directly especially in the infrared due to foreground contamination [5].

With the advent of imaging air Cherenkov telescopes (IACTs) that are able to observe very high energy (energy $E \gtrsim 100$ GeV, VHE) γ-rays from distant sources it is possible to place upper limits on the intensity of the EBL under the assumption of a certain intrinsic source spectrum. VHE γ-rays can interact with EBL photons and produce electron-positron pairs. These γ-rays are thus removed from the photon beam and initial photon flux of the source, $\mathrm{d}N_{\mathrm{int}}/\mathrm{d}E$, is attenuated. This is commonly expressed as

$$\frac{\mathrm{d}N_{\mathrm{obs}}}{\mathrm{d}E} = \frac{\mathrm{d}N_{\mathrm{int}}}{\mathrm{d}E} \times \exp\left[-\tau_{\gamma\gamma}(E,z)\right], \tag{1}$$

where the observed spectrum is denoted by $\mathrm{d}N_{\mathrm{obs}}/\mathrm{d}E$. The parameter $\tau_{\gamma\gamma}$ is called the optical depth and is a three-fold integral over the cosmological distance to the source at redshift z_0, the cosine of the angle

of incidence of the photons μ, and the energy ϵ of the background photons [6],

$$\tau_{\gamma\gamma}(E, z_0) = \int_0^{z_0} \mathrm{d}\ell(z) \int_{-1}^{+1} \mathrm{d}\mu \frac{1-\mu}{2} \int_{\epsilon'_{\mathrm{thr}}}^{\infty} \mathrm{d}\epsilon' n_{\mathrm{EBL}}(\epsilon', z) \sigma_{\gamma\gamma}(E', \epsilon', \mu). \tag{2}$$

The comoving photon number density of the EBL in the energy interval ϵ' and $\mathrm{d}\epsilon'$ at redshift z enters as n_{EBL} and the cross section for pair production as $\sigma_{\gamma\gamma}$. The threshold energy for pair production is given by $\epsilon'_{\mathrm{thr}} = \epsilon_{\mathrm{thr}}(E', \mu)$ with $E' = E(1+z)$. The cross section is strongly peaked at a wavelength $\lambda = 1.24(E/\mathrm{TeV})$ μm, making the EBL the dominant background for the attenuation of VHE photons.

Several authors have used VHE spectra measured by IACTs to constrain the EBL [7, 8, 9, 10]. In [7] the authors test a great variety of shapes of the EBL intensity. For each shape they calculate the absorption and correct the observed VHE spectra accordingly. Subsequently, they compare the obtained intrinsic spectra with theoretical predictions, i.e. if the intrinsic spectra are described with power laws, $\mathrm{d}N_{\mathrm{int}}/\mathrm{d}E \propto E^{-\Gamma}$, with $\Gamma < 1.5$ or if the spectra are best described with an exponential pile up at the highest energies. If one of the two conditions is true the corresponding EBL shape is excluded. The envelope shape of allowed shapes gives the upper limit of the EBL intensity.

This article follows the same approach but its goal is to examine the consequences on the EBL upper limits if the evolution is not neglected but implemented in a phenomenological way outlined by [11]. However, the value of $\Gamma = 1.5$ as a limit is somewhat under debate. Harder spectra, i.e. spectral indices $\Gamma < 1.5$, can be achieved e.g. in the case of internal photon absorption [12], proton-synchrotron radiation [13, 14] or narrow electron injection spectra [15, 16, 17]. In this work, the focus lies on the influence of the evolution with redshift on upper limits of the EBL intensity. Thus, the limiting value of 1.5 is chosen for simplicity and to compare the results to [7].

2. Method of constraining the EBL density with VHE observations

2.1. Calculating the EBL photon density

Following [7], the EBL SED νI_ν (in nW m^{-2} sr^{-1}) is described by splines,

$$\nu I_\nu = \sum_{i=0}^{k} w_i s_{i,p}(\epsilon) \tag{3}$$

with the B-Splines $s_{i,p}$,

$$s_{i,0}(\epsilon) = \begin{cases} 1 & \epsilon_i \le \epsilon < \epsilon_{i+1} \text{ and } \epsilon_i < \epsilon_{i+1}, \\ 0 & \text{otherwise,} \end{cases} \tag{4}$$

$$s_{i,p}(\epsilon) = \frac{\epsilon - \epsilon_i}{\epsilon_{i+1} - \epsilon_i} s_{i,p-1}(\epsilon) + \frac{\epsilon_{i+p+1} - \epsilon}{\epsilon_{i+p+1} - \epsilon_{i+p}} s_{i+1,p-1}(\epsilon), \tag{5}$$

and the order p is set to two. Each spline is defined by the choice of k supporting points in the (λ,νI_ν)-plane, where λ, $i = 1, \ldots, k$ are the knot points and w_i are the weights of the spline. For the knot points 16 equidistant points in $\log_{10}(\lambda)$ between 0.1 and 1000 μm are chosen and 12 equidistant points of the EBL density in $\log_{10}(\nu I_\nu)$ between 0.06 and 100 nW m^2 sr^{-1} are set as weights. It should be stressed that the splines will in general not run through each weight and knot. The grid defined by the selection of weights and knots is limited by an envelope shape, which is shown in Figure 1. The minimum allowed shape is set to reproduce the lower limits from the galaxy number counts from Spitzer [18] while the maximum allowed shape roughly follows the measurements and upper limits. In total this range of knots and weights allows for 518,400 different EBL shapes.

Assuming the EBL intensity is constant in redshift, the differential photon number density is given by [20]

$$n_{\mathrm{EBL}}(\epsilon, z) = \frac{4\pi}{c\epsilon^2} (1+z)^2 \nu I_\nu(\epsilon = h\nu). \tag{6}$$

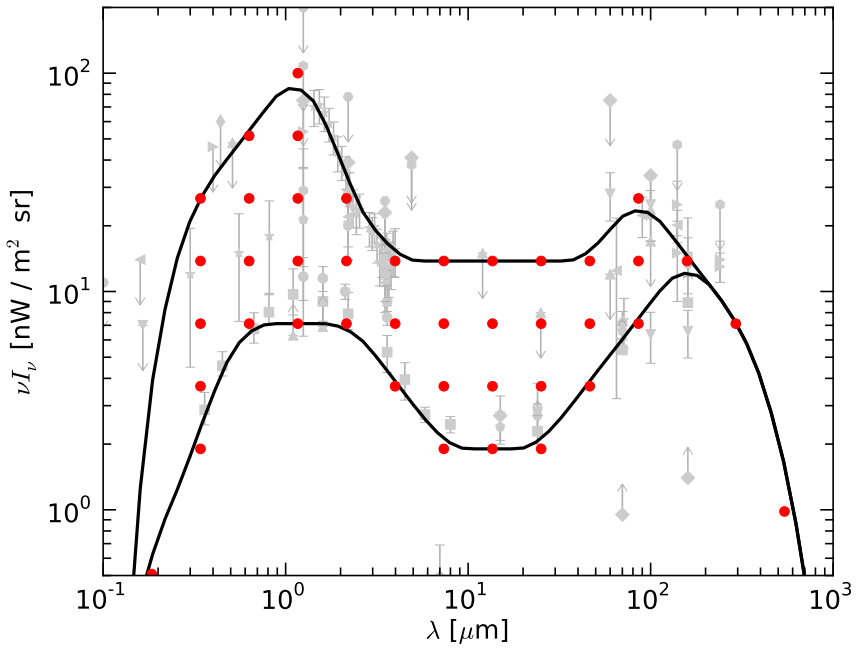

Figure 1. Grid points that are used to construct EBL shapes. The points are shown in red together with the minimal and maximal shape depicted as black lines. Direct measurements as well as lower and upper limits on the EBL are shown in gray [19].

However, the evolution of stars, dust and galaxies with redshift leads to an evolution of the EBL with redshift as well. This is also implemented in the modeling of the EBL (see e.g. [21, 20, 22]). Here, it is accounted for with the phenomenological ansatz of [11]. The cosmological photon number density scaling is changed from $n_{\rm EBL} \propto (1+z)^2$ to $n_{\rm EBL} \propto (1+z)^{2-f_{\rm evo}}$. For a value of $f_{\rm evo} = 1.2$ a good agreement is found (the deviation in $\tau_{\gamma\gamma}$ is found to be $< 4\%$ for $z = 0.2$ and $< 10\%$ for $z = 0.5$) for redshifts $z \lesssim 0.7$ between this simplified approach and complete EBL model calculations [11]. On the other hand, neglecting the evolution entirely leads to an overestimation of the optical depth between 10% ($z = 0.2$) and 35% ($z = 0.5$). Thus, including the evolution will generally weaken the upper limits on the EBL energy density.

2.2. Exclusion criteria

The derivation of upper limits is limited here to the three spectra, namely measurements of the sources H1426-428 [23] (measured by HEGRA), 1ES1101-232 [24] (observed with H.E.S.S.) and 3C279 [25] (measured by MAGIC). If an EBL shape is excluded is determined in the same fashion as in [7]. For a particular EBL shape the intrinsic spectrum is calculated by inverting Eq. 1. Subsequently, analytical functions (given in Table 2 of [7]) are fitted to the data points. An EBL shape is excluded if one of the following conditions is met:

(i) The photon index (or one of the photon indices if the spectrum is best described with a (double) broken power law) Γ of the analytical function is smaller than 1.5,

$$\Gamma + \sigma_\Gamma + \sigma_{\rm sys} < 1.5, \tag{7}$$

where σ_Γ is the uncertainty associated with the fitting procedure and $\sigma_{\rm sys}$ is the systematic error of the photon index quoted in the corresponding reference.

(ii) The spectrum is best described with a function that contains an exponential pile up at the largest energies.

	Source			
	H1426+428	1ES1101-232	3C279	Combined
With evolution	13.91%	21.50%	58.78%	0.93%
W/o evolution	13.05%	17.78%	49.61%	0.60%

Table 1. Percentage of allowed shapes for each spectrum with and without evolution. The numbers show that if evolution is neglected up to 10% (3C279) more shapes are excluded.

The upper limit EBL shape is defined as the envelope shape of all allowed shapes.

3. Results

The upper limits are derived using the three VHE spectra from the sources H1426+428 [23], 1ES1101-232 [24] and 3C279 [25]. The first two spectra are included in the analysis of [7]. The sources are located at redshifts of 0.129, 0.186 and 0.536 respectively and thus a weakening of the upper limits due to the inclusion of the evolution of the EBL can be expected. This is seen in Figure 2 which shows a comparison of the limits with and without evolution together with the limits derived in [7]. For completeness, two EBL models are shown as well. The blue solid line indicates the limits with evolution which are indeed weaker than those derived without evolution (dark blue dashed curve). The differences are most prominent in the transition at near infrared wavelengths where 1ES1101-232 and 3C279 give the most constraining limits which can be inferred from the strongly peaked cross section for pair production and the energy ranges covered by the spectra. This is natural as the effect of the evolution becomes more pronounced for higher redshifts. Table 1 lists the ratio of the number of allowed shapes to the total number of shapes for each spectrum with and without evolution.

The deviations from the upper limits of [7] can be explained, on the one hand, by the slightly different choice of the grid for the splines. In the present analysis the grid is shifted towards lower values of the intensity along the y-axis (see Figure 1) in order to cover the lower limits from galaxy counts. The spectrum of Markarian 501 [26] which excludes most EBL shapes in [7] is not considered here since the evolution should only have a negligible impact on this spectrum as the source is relatively close by with $z = 0.034$. On the other hand, the previously unconsidered source 3C279 improves the upper limits at optical wavelengths.

4. Conclusions

In this paper the effect of the evolution of the EBL density with redshift on upper limits from VHE observations is studied. The evolution is implemented in the phenomenological way outlined in [11]. The expectation is confirmed that the evolution generally weakens the upper limits since the photon number density of the EBL is reduced. The result underlines the necessity to include this effect in upper-limit calculations which has not been done so far. Furthermore, new upper limits from the source 3C279 are presented that improve the upper limits of [7] in the optical by roughly a factor of 2.

Acknowledgements

The authors would like to thank the organizers of the conference *Beamed and unbeamed gamma rays from galaxies* 2011 for the opportunity to present the results of this work. This work was made possible with the support of the state excellence cluster "Cosmic radiation fields and search for dark matter" at the university of Hamburg.

References

[1] Hauser M G and Dwek E 2001 *Ann. Rev. Astron. Astrophys.* **39** 249–307 (*Preprint* arXiv:astro-ph/0105539)
[2] Matute I, La Franca F, Pozzi F, Gruppioni C, Lari C and Zamorani G 2006 *Astron. Astrophys.* **451** 443–456 (*Preprint* arXiv:astro-ph/0601355)

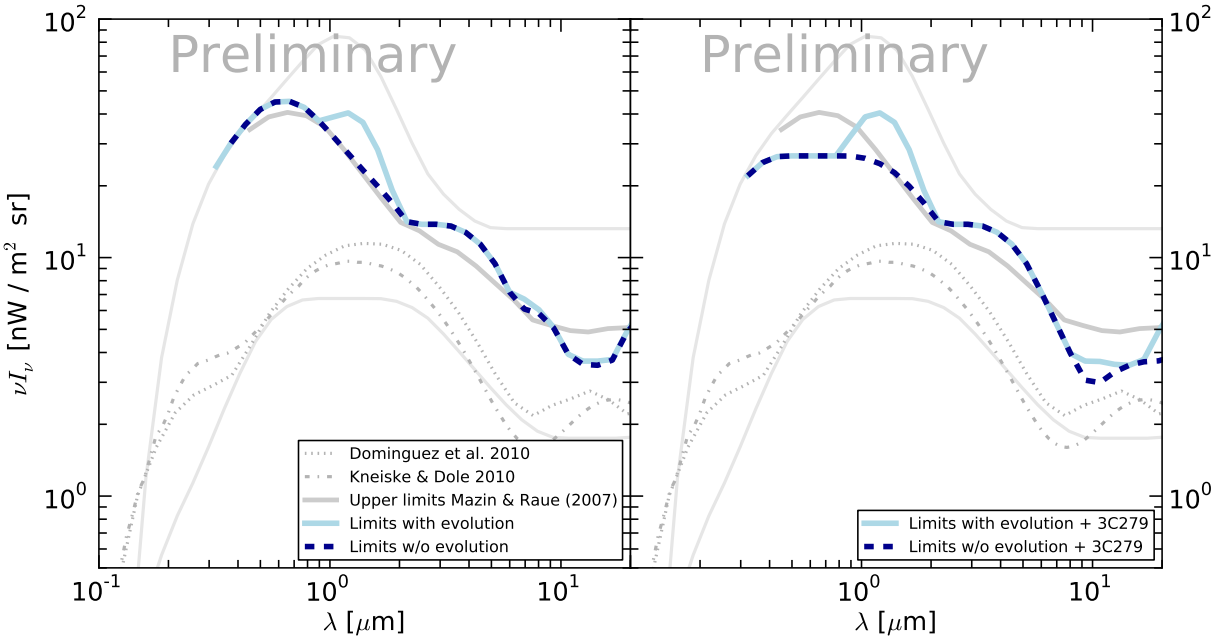

Figure 2. Upper limits with and without evolution. As a comparison the EBL models of [21] and [22] are shown together with the limits of [7].

[3] Raue M, Kneiske T and Mazin D 2009 *Astron. Astrophys.* **498** 25–35 (*Preprint* 0806.2574)
[4] Maurer A, Raue M, Kneiske T, Elsässer D, Hauschildt P and Horns D 2011 *in preperation*
[5] Hauser M G, Arendt R G, Kelsall T, Dwek E, Odegard N, Weiland J L, Freudenreich H T, Reach W T, Silverberg R F, Moseley S H, Pei Y C, Lubin P, Mather J C, Shafer R A, Smoot G F, Weiss R, Wilkinson D T and Wright E L 1998 *Astrophys. J.* **508** 25–43 (*Preprint* arXiv:astro-ph/9806167)
[6] Gould R J and Schréder G P 1967 *Physical Review* **155** 1404–1407
[7] Mazin D and Raue M 2007 *Astron. Astrophys.* **471** 439–452 (*Preprint* arXiv:astro-ph/0701694)
[8] Georganopoulos M, Finke J D and Reyes L C 2010 *Astrophys. J., Lett.* **714** L157–L161 (*Preprint* 1004.0017)
[9] Mankuzhiyil N, Persic M and Tavecchio F 2010 *Astrophys. J., Lett.* **715** L16–L20 (*Preprint* 1004.2032)
[10] Orr M R, Krennrich F and Dwek E 2011 *Astrophys. J.* **733** 77–+ (*Preprint* 1101.3498)
[11] Raue M and Mazin D 2008 *International Journal of Modern Physics D* **17** 1515–1520 (*Preprint* 0802.0129)
[12] Aharonian F A, Khangulyan D and Costamante L 2008 *Mon. Not. R. Astron. Soc.* **387** 1206–1214 (*Preprint* 0801.3198)
[13] Aharonian F A 2000 *New Astronomy* **5** 377–395 (*Preprint* arXiv:astro-ph/0003159)
[14] Zacharopoulou O, Khangulyan D, Aharonian F A and Costamante L 2011 *Astrophys. J.* **738** 157–+ (*Preprint* 1106.3129)
[15] Katarzyński K, Ghisellini G, Tavecchio F, Gracia J and Maraschi L 2006 *Mon. Not. R. Astron. Soc.* **368** L52–L56 (*Preprint* arXiv:astro-ph/0603030)
[16] Tavecchio F, Ghisellini G, Ghirlanda G, Costamante L and Franceschini A 2009 *Mon. Not. R. Astron. Soc.* **399** L59–L63 (*Preprint* 0905.0899)
[17] Lefa E, Rieger F M and Aharonian F 2011 *ArXiv e-prints* (*Preprint* 1106.4201)
[18] Fazio G G, Ashby M L N, Barmby P, Hora J L, Huang J S, Pahre M A, Wang Z, Willner S P, Arendt R G, Moseley S H, Brodwin M, Eisenhardt P, Stern D, Tollestrup E V and Wright E L 2004 *Astrophys. J., Suppl. Ser.* **154** 39–43 (*Preprint* arXiv:astro-ph/0405595)
[19] Raue M and Mazin D 2011 *ArXiv e-prints* (*Preprint* 1106.4384)
[20] Franceschini A, Rodighiero G and Vaccari M 2008 *Astron. Astrophys.* **487** 837–852 (*Preprint* 0805.1841)
[21] Domínguez A, Primack J R, Rosario D J, Prada F, Gilmore R C, Faber S M, Koo D C, Somerville R S, Pérez-Torres M A, Pérez-González P, Huang J S, Davis M, Guhathakurta P, Barmby P, Conselice C J, Lozano M, Newman J A and Cooper M C 2011 *Mon. Not. R. Astron. Soc.* **410** 2556–2578 (*Preprint* 1007.1459)
[22] Kneiske T M and Dole H 2010 *Astron. Astrophys.* **515** A19+ (*Preprint* 1001.2132)
[23] Aharonian (for the HEGRA Collaboration) F *et al.* 2003 *Astron. Astrophys.* **403** 523–528 (*Preprint* arXiv:astro-ph/0301437)
[24] Aharonian (for the HESS Collaboration) F *et al.* 2007 *Astron. Astrophys.* **470** 475–489 (*Preprint* 0705.2946)
[25] MAGIC Collaboration *et al.* 2008 *Science* **320** 1752– (*Preprint* 0807.2822)

[26] Aharonian (for the HEGRA Collaboration) F A *et al.* 1999 *Astron. Astrophys.* **349** 11–28 (*Preprint* arXiv:astro-ph/9903386)